Title	Modelling the effect of density on the unimodal soil-water characteristic curve
Author(s)	Wijaya, M.; Leong, Eng Choon
Citation	Wijaya, M., & Leong, E. C. (2017). Modelling the effect of density on the unimodal soil-water characteristic curve. Géotechnique, 67(7), 637-645.
Date	2017
URL	http://hdl.handle.net/10220/43606
Rights	© 2017 ICE Publishing. This paper was published in Géotechnique and is made available as an electronic reprint (preprint) with permission of ICE Publishing. The published version is available at: [http://dx.doi.org/10.1680/jgeot.15.P.270]. One print or electronic copy may be made for personal use only. Systematic or multiple reproduction, distribution to multiple locations via electronic or other means, duplication of any material in this paper for a fee or for commercial purposes, or modification of the content of the paper is prohibited and is subject to penalties under law.

Wijaya, M. & Leong, E. C. (2017). *Géotechnique* **67**, No. 7, 637–645 [http://dx.doi.org/10.1680/jgeot.15.P.270]

TECHNICAL NOTE

Modelling the effect of density on the unimodal soil-water characteristic curve

M. WIJAYA* and E. C. LEONG†

Research has shown that the soil-water characteristic curve (SWCC) is dependent on the density of the soil; therefore, using a single SWCC based on one density is insufficient to describe the SWCC of soil in the field, which may have significant density variation. In order to take into account the effect of density on the SWCC, soils of different densities need to be tested, and this is impractical. In this note, an equation which can account for the effect of density on a unimodal SWCC plotted in terms of gravimetric water content by determining only one SWCC is proposed. The proposed equation was verified using data from this study as well as other published data.

KEYWORDS: clays; laboratory tests; sands; silts; suction

INTRODUCTION

The soil-water characteristic curve (SWCC) describes the relationship between matric suction and water content (Williams, 1982; Fredlund & Rahardjo, 1993) and has been heavily utilised to characterise the behaviour of unsaturated soils (Wijaya *et al.*, 2015). The water content in the SWCC can be represented by either gravimetric water content, w, volumetric water content, θ_w, or degree of saturation, S_r. An SWCC can be either unimodal or bimodal, with the former being more common. A typical unimodal SWCC when plotted with gravimetric water content (SWCC-w), the subject of this note, is given in Fig. 1(a). In Fig. 1(a), the SWCC-w is divided into three linear segments: the initial drying line, virgin drying line and residual drying line. When SWCC is plotted with degree of saturation (SWCC-S), the three linear segments are called the saturation line, virgin desaturation line and residual desaturation line, as shown in Fig. 1(b).

A number of equations have been proposed to fit the unimodal SWCC. The parameters of the equations were obtained by curve fitting. Efforts have also been made to correlate these empirical parameters with other soil properties (e.g. Chin *et al.*, 2010). For bimodal SWCCs, three approaches are commonly used to curve fit the bimodal SWCC (Wijaya & Leong, 2016), namely, the piecewise approach (Smettem & Kirkby, 1990; Wilson *et al.*, 1992; Burger & Shackelford, 2001), fraction of total volume approach (Othmer *et al.*, 1991; Ross & Smettem, 1993; Durner, 1994; Mallants *et al.*, 1997; Zhang & Chen, 2005) and the unique parameter approach (Gitirana & Fredlund, 2004; Li, 2009; Satyanaga *et al.*, 2013; Li *et al.*, 2014; Wijaya & Leong, 2016).

Each SWCC equation has its own advantages. For example, the Gitirana & Fredlund (2004) equation is able to curve fit both unimodal and bimodal SWCCs by using empirical parameters. However, the Gitirana & Fredlund (2004) equation is only valid for SWCC-S, where the slope of the first segment of the SWCC-S is assumed to be zero, as degree of saturation is 1 from zero matric suction up to the air-entry value. However, the slope of the first segment for SWCC-w is not zero. A more thorough discussion on each SWCC equation is provided in Wijaya & Leong (2016).

The soil dry density, which can be represented by the saturated water content w_{sat}, void ratio e, or relative density D_r, affects the SWCC. Therefore, it is not appropriate to use a single SWCC for soils with various dry densities. The effect of soil dry density on the SWCC also depends on whether the SWCC is plotted based on gravimetric water content (Jotisankasa *et al.*, 2007; Salager *et al.*, 2010, 2011) or degree of saturation (Huang *et al.*, 1998; Gallipoli *et al.*, 2003; Jotisankasa *et al.*, 2007; Nuth & Laloui, 2008; Tarantino, 2009; Sheng & Zhou, 2011; Zhou *et al.*, 2014). Salager *et al.* (2010) found that a decrease in initial dry soil density causes a decrease in saturated gravimetric water content and therefore affects only the initial segment of the SWCC-w. However, the SWCC-w of the same soil at various initial dry densities merges into the virgin drying line and residual line, as shown in Fig. 1(a). For SWCC-S, a decrease in the initial dry density causes the AEV to increase from AEV_0 to AEV_f, such that the SWCC-S shifts to the right, as shown in Fig. 1(b). Therefore, a higher matric suction is required to reach the same degree of saturation (Huang *et al.*, 1998; Gallipoli *et al.*, 2003; Tarantino & Tombolato, 2005; Jotisankasa *et al.*, 2007; Nuth & Laloui, 2008; Tarantino, 2009; Sheng & Zhou, 2011; Zhou *et al.*, 2014).

Both water content and void ratio change with matric suction independently and are unique for different soils (Wijaya *et al.*, 2015). As a result, modelling the effect of density on SWCC-S requires both the SWCC-w and the shrinkage curve, which makes SWCC-S different for different initial dry densities, as shown in Fig. 1(b). It is important to note that s_2 in SWCC-w is not AEV in SWCC-S, as AEV can only be determined from SWCC-S (Wijaya *et al.*, 2015).

Thus, modelling the effect of density on SWCC-w is easier, as the unknown is only located prior to the virgin drying line

Manuscript received 11 December 2015; revised manuscript accepted 20 December 2016. Published online ahead of print 23 January 2017.
Discussion on this paper closes on 1 December 2017, for further details see p. ii.
* School of Civil and Environmental Engineering, Nanyang Technological University, Singapore.
† School of Civil and Environmental Engineering, Nanyang Technological University, Singapore (Orcid: 0000-0002-0941-0984).

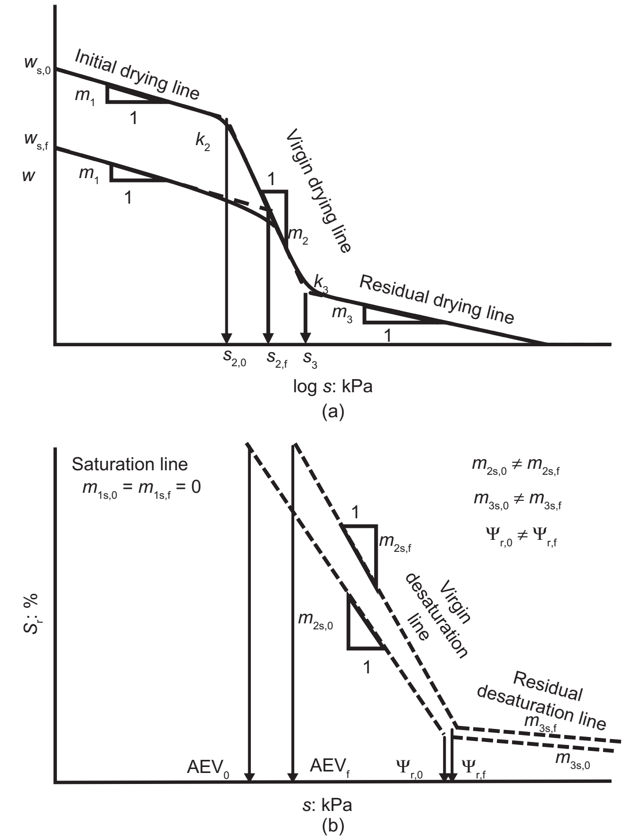

Fig. 1. SWCC and definition of parameters: (a) SWCC-w under different density; (b) SWCC-S under different density

(Fig. 1(a)). However, for soil which does not change in volume due to an increase in matric suction, SWCC-S can be directly obtained from SWCC-w, as the initial void ratio e_0 remains unchanged. Thus, the focus of this note is to develop a method to estimate SWCC-w by using only one SWCC test. When the effect of initial dry density on the shrinkage curve can be established, the proposed model can be easily extended to estimate SWCC-S.

Several equations have been proposed to account for the effect of density on the SWCC-w and SWCC-S, as shown in Table 1. The Zhou *et al.* (2014) equation uses initial porosity n_0 to directly describe the effect of density on the SWCC-S and therefore has a significant advantage compared to the other equations in Table 1 as it requires only one test to obtain all of the parameters. Tarantino (2009) proposed an equation to determine the SWCC-S where all of the parameters can be determined from one test, but it requires the instantaneous void ratio data, which at times are not available in the SWCC-w measurement. The Gallipoli *et al.* (2003), Zhou *et al.* (2012) and Salager *et al.* (2010) equations can take account of the effect of density on the SWCC but this requires an additional test and thus can be considered as less advantageous compared to the Zhou *et al.* (2014) and Tarantino (2009) equations.

Wijaya & Leong (2016) developed an equation that can conveniently model both unimodal and bimodal SWCCs by using transition functions, T_i. The equation parameters can be graphically obtained. The Wijaya & Leong (2016) equation in compact form is given as follows

$$T_i(x, x_1, x_i, m_i, m_{i-1}, k_i) = \frac{1}{2}(m_i - m_{i-1})\left\langle (x - x_1) + \frac{1}{k_i}\ln\left\{\frac{\cosh[k_i(x - x_i)]}{\cosh[k_i(x_i - x_1)]}\right\}\right\rangle \quad (1)$$

$$w(s) = f_1 - \sum_{i=2}^{n} T_i(\log s, \log s_1, \log s_i, m_i, m_{i-1}, k_i) \quad (2)$$

$$f_1 = w_s - m_1 \log\frac{s}{s_1} \quad (3)$$

where m_i is the slope of the linear segment i; s_i is the matric suction at the intersection between segment i and segment $i-1$; k_i is the curvature parameter between segment i and segment $i-1$; w_s is the saturated gravimetric water content; m_1 is the slope of the initial drying line; and s_1 is the matric suction at w_s. For unimodal SWCC, $n = 3$, whereas for bimodal SWCC, $n = 5$. The equation for unimodal SWCC-w in expanded form is given as

$$w(s) = w_s - m_1 \log\frac{s}{s_1} - T_2(\log s, \log s_1, \log s_2, m_2, m_1, k_2) - T_3(\log s, \log s_1, \log s_3, m_3, m_2, k_3) \quad (4)$$

where m_2 is the slope of the virgin drying line; m_3 is the slope of residual drying line; k_2 is the curvature parameter between segments 1 and 2; k_3 is the curvature parameter between segments 2 and 3; s_2 is the matric suction at the intersection between the virgin drying line and the initial drying line; and s_3 is the residual matric suction (Fig. 1(a)). In this study, the Wijaya & Leong (2016) equation was extended to show how density can be accounted for in the SWCC-w by only determining one SWCC-w to obtain the parameters.

EXPERIMENTAL PROCEDURE AND RESULTS

Two types of soils were prepared. The first type of soil is a sand sample (100% sand fraction) from a reclamation site. The properties of the sand are shown in Table 2. The SWCCs of the sand specimens were obtained by using Tempe cell following ASTM-D6836-02 (ASTM, 2008) standard procedure method C.

A summary of the SWCC tests on sand specimens is given in Table 3. Based on Fig. 2, the higher the relative density of the sand specimen, the higher the value of s_2. However, once the matric suction exceeds the s_2, the curve merges into the virgin drying line. The matric suction s_3 and the slope of the residual line m_3 appear to be unaffected by the difference in relative densities.

The second type of soil is a kaolin sample, which was prepared from a slurry. Kaolin was mixed with water into a slurry and then consolidated under a consolidation pressure of 150 kPa. The kaolin has a specific gravity G_s of 2·66. The consolidated kaolin sample has a water content w_{sat} of 61·2%. Two kaolin specimens were prepared. The kaolin specimens were first obtained from the kaolin sample using a cutting ring with an internal diameter of 6·3 cm. One of the kaolin specimens was loaded in an oedometer up to 2035 kPa and then unloaded. The resulting kaolin specimen (specimen 2) has w_{sat} of 44·3%. The SWCC-w of the kaolin specimens were obtained by using the pressure plate apparatus following ASTM-D6836-02 (ASTM, 2008) standard procedure method C. For completeness of the SWCC-w, chilled-mirror dew-point test were conducted following ASTM-D6836-02 (ASTM, 2008) standard procedure method D to obtain the SWCC data points with matric suction higher than 1000 kPa.

A similar observation of the SWCC-w for the sand specimens was obtained for the kaolin specimens where the SWCC-w merged at the virgin drying line. The chilled-mirror dew-point test results indicate that even a kaolin specimen

Table 1. Models of SWCC

Author	Equation	Parameters
Gallipoli *et al.* (2003) – modified Van Genuchten (1980) equation	$S_r = \left\{\frac{1}{1+[s\phi(e)^{\psi}]^{n_g}}\right\}^{m_g}$ ϕ and Ψ require additional SWCCs to be determined	w = gravimetric water content w_{sat} = saturated gravimetric water content S_r = degree of saturation n_0 = initial porosity e = void ratio e_0 = initial void ratio s = matric suction s_r = residual matric suction s_p = matric suction of virgin drying line at 0 water content m_2 = slope of virgin drying line a_f, n_f, m_f = Fredlund & Xing (1994) curve-fitting parameters n_g, m_g = Van Genuchten (1980) curve-fitting parameters A_s, B_s = Salager *et al.* (2010) curve-fitting parameters ϕ, ψ = Gallipoli *et al.* (2003) curve-fitting parameters A_t, B_t = Tarantino (2009) curve-fitting parameters ζ = Zhou *et al.* (2012) curve-fitting parameters
Tarantino (2009) – Van Genuchten (1980) equation	$S_r = \left\{1+\left[\left(\frac{e}{A_t}\right)^{1/B_t} s\right]^{n_g}\right\}^{-B_t/n_g}$	
Salager *et al.* (2010) – modified Fredlund & Xing (1994) equation	$w = \frac{w_{sat}}{\{\ln[\exp(1)+(s/a_f)^{n_f}]\}^{m_f}}\left\{1-\frac{\ln[1+(s/s_r)]}{\ln[1+(10^6/s_r)]}\right\}$ $m_f = 3{\cdot}67\ln\left\langle\frac{w_{sat}}{m_2\ln(s_p/a_f)}\left\{1-\frac{\ln[1+(a_f/s_r)]}{\ln[1+(10^6/s_r)]}\right\}\right\rangle$ $n_f = 3{\cdot}72\frac{1\cdot 31^{m_f+1}}{m_f\{1-\ln[1+(a_f/s_r)]/\ln[1+(10^6/s_r)]\}}$ $\left\{\frac{m_2}{w_{sat}}-\frac{a_f}{1\cdot 31^{m_f}(a_f+s_r)\ln[1+(10^6/s_r)]}\right\}$ $a_f = A_S e_0^{B_S}$ A_s and B_s require additional SWCCs to be determined	
Zhou *et al.* (2012)	$S_e = -\int\frac{S_e}{e_i}(1-S_e)^{\zeta}\mathrm{d}e_i$ S_e is determined from other SWCC equation. Solution based on Simpson's rule is given as $\ln\frac{e_f}{e_i}\approx\frac{S_{e,f}-S_{e,0}}{6}[f(S_{e,0})]+4f\left(\frac{S_{e,0}+S_{e,f}}{2}\right)+f(S_{e,f})$ $f(x)=\frac{1}{x(1-x)^{\zeta}}$ ζ requires additional SWCCs to be determined	
Zhou *et al.* (2014) – modified Fredlund & Xing (1994) equation	$S_r = \frac{1}{\{\ln[\exp(1)+(sn_0/a_f)^{n_0n_f}]\}^{n_0m_f}}\left\{1-\frac{\ln[1+(s/s_r)]}{\ln[1+(10^6/s_r)]}\right\}$ $w = \frac{e}{G_s\{\ln[\exp(1)+(sn_0/a_f)^{n_0n_f}]\}^{n_0m_f}}\left\{1-\frac{\ln[1+(s/s_r)]}{\ln[1+(10^6/s_r)]}\right\}$	

Table 2. Properties of sand

Parameter	Value
G_s	2·64
$\rho_{dry\text{-}minimum}$: t/m^3	1·352
$\rho_{dry\text{-}maximum}$: t/m^3	1·736
e_{min}	0·518
e_{max}	0·949

Table 3. Summary of SWCC tests on sand specimens

Name	w_f: %	w_0	e_0	D_r: %
S1	1·74	20·40	0·538	95·50
S2	1·82	26·13	0·689	60·43
S3	1·68	24·69	0·651	69·25
S4	1·79	25·97	0·685	61·37
S5	1·95	24·13	0·636	72·67

which was broken into smaller pieces for the chilled-mirror dew-point test has an SWCC-w with a unique virgin drying line.

MODELLING THE EFFECT OF DENSITY ON THE SWCC

The density of a soil can be represented as a function of e_0, w_s or D_r. The behaviour of sand is commonly related to its D_r. Equation (3) implicitly describes the density of soil using parameter w_s. When e_0 is used to describe the density of the soil, equation (3) becomes

$$f_1 = \frac{S_r e_0}{G_s} - m_1 \log\frac{s}{s_1} \tag{5}$$

Equation (5) can be easily modified to model the effect of relative density on the SWCC of sand. The relative density of the sand specimen is given as follows

$$D_r = \frac{e_{max}-e}{e_{max}-e_{min}} \tag{6}$$

By using equation (6), it is possible to describe e in terms of e_{max}, e_{min} and D_r as follows

$$e = e_{max}(1-D_r) + e_{min}D_r \tag{7}$$

The saturated water content of the sand specimen w_s can be described in term of D_r using

$$w_s = \frac{S_r}{G_s}[e_{max}(1-D_r)+e_{min}D_r] \tag{8}$$

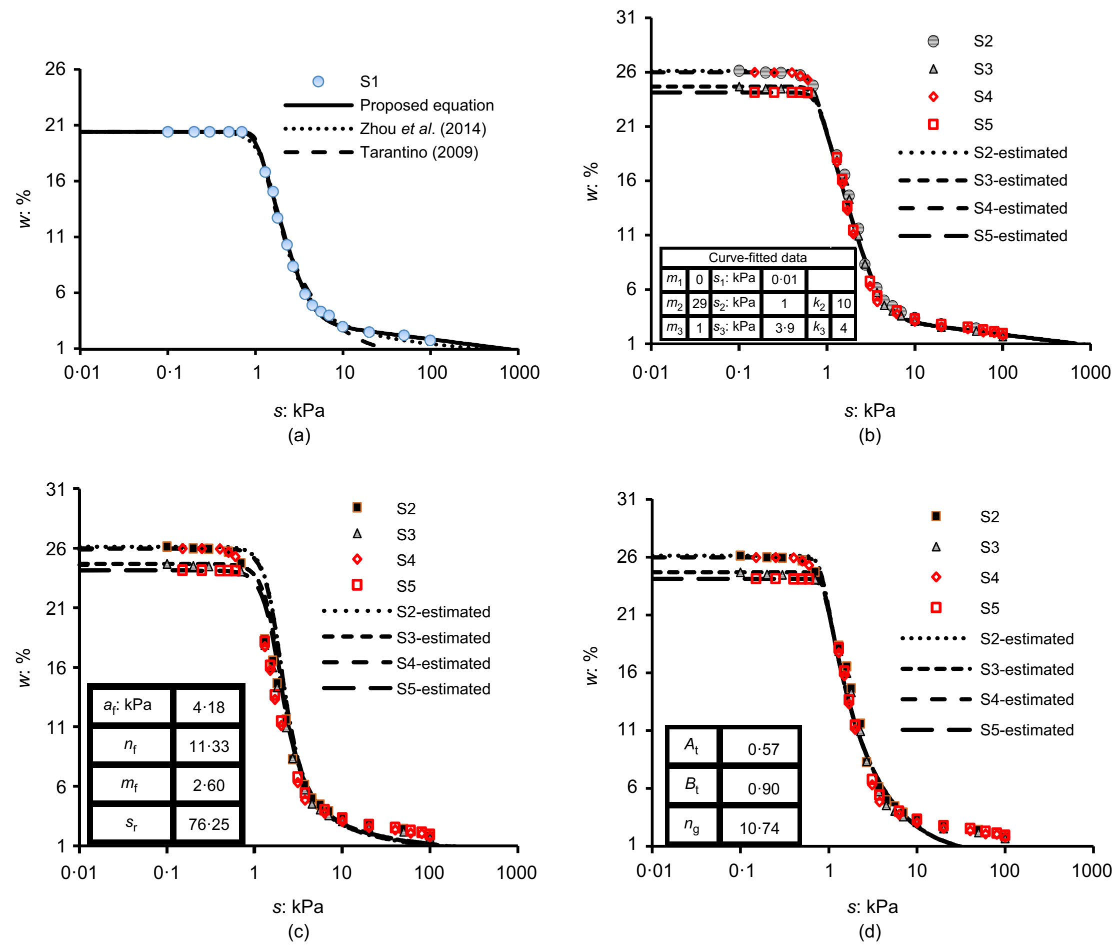

Fig. 2. Results of proposed equation in estimating SWCC-w for specimens S2, S3, S4 and S5 by using data from specimen S1: (a) calibrated SWCC-w; (b) proposed equation; (c) Zhou *et al.* (2014) equation; (d) Tarantino (2009) equation

Substituting w_s in equation (8) into equation (3) will give

$$f_1 = \frac{S_r}{G_s}[e_{max}(1 - D_r) + e_{min}D_r] - m_1 \log\frac{s}{s_1} \qquad (9)$$

Equation (9) accounts for the effect of D_r on the w_s of the sand specimen. However, it does not account for the changes in the s_2 that will also change due to the change in D_r. The effect of D_r on s_2 is described in Fig. 1(a). Increasing D_r will decrease w_s from $w_{s,0}$ to $w_{s,f}$. The slopes, m_1 and m_2 are assumed to be constant. Using Fig. 1, it is possible to relate $s_{2,f}$ with $s_{2,0}$, $w_{s,0}$, $w_{s,f}$ and m_2 as follows

$$s_{2,f} = s_{2,0} \times 10^{\left(w_{s,0} - w_{s,f}\right)/(m_2 - m_1)} \qquad (10)$$

Modification of equation (4) can therefore be done by replacing f_1 in equation (2) with f_1 in equation (9), and substituting $s_2 = s_{2,f}$ in equation (10) into equation (2) to give

$$w(s) = \frac{S_r}{G_s}[e_{max}(1 - D_r) + e_{min}D_r] - m_1 \log\frac{s}{s_1} - T_2\Big(\log s, \log s_1, \log s_2 = \log\Big\{s_{2,0} \times 10^{w_{s,0} - (S_r/G_s)[e_{max}(1-D_r) + e_{min}D_r]/(m_2 - m_1)}\Big\}, m_2, m_1, k_2\Big) - T_3(\log s, \log s_1, \log s_3, m_3, m_2, k_3) \qquad (11)$$

When D_r is not available, equation (5) can be used to replace f_1 in equation (2). Substituting equations (5) and (10) into equation (2), the SWCC equation which takes into account the effect of initial void ratio on the SWCC is given as

$$w(s) = \frac{S_r}{G_s}e_0 - m_1 \log\frac{s}{s_1} - T_2\Big(\log s, \log s_1, \log\Big\{s_{2,0} \times 10^{[w_{s,0} - (S_r e_0/G_s)]/(m_2 - m_1)}\Big\}, \times m_2, m_1, k_2\Big) - T_3(\log s, \log s_1, \log s_3, m_3, m_2, k_3) \qquad (12)$$

In equations (11) and (12), k_2 and k_3 are assumed to be constant regardless of the difference in D_r or e.

VERIFICATION OF THE PROPOSED EQUATION

In order to estimate the SWCC-w of sand specimens S2 to S5, only the SWCC-w of sand specimen S1 is required. In Fig. 2(a), m_1, m_2, m_3, k_2, k_3, s_1, $s_2 = s_{2,0}$ and s_3 were determined from the SWCC-w of sand specimen S1. Equation (11) was then used to estimate the

SWCC-w of the sand specimens S2 to S5 as shown in Fig. 2(b).

The estimated SWCC-w in Fig. 2(b) shows that equation (11) works very well. The Zhou *et al.* (2014) and Tarantino (2009) equations shown in Table 1 can also be used to estimate SWCC-w of sand specimens S2 to S5 by using only the SWCC-w of sand specimen S1 to obtain the parameters as shown in Figs 2(a), 2(c) and 2(d).

Therefore, the Zhou *et al.* (2014) and Tarantino (2009) equations were compared with the proposed equation. As both of the equations used degree of saturation, the gravimetric water content for both equations was obtained following the basic soil properties relationship between w, e and specific gravity G_s. For the Tarantino (2009) equations, the instantaneous void ratio is replaced with initial void ratio. Figures 2(c) and 2(d) show the estimated SWCC-w by using the Zhou *et al.* (2014) and Tarantino (2009) equations. Two noticeable weaknesses can be seen from both equations. The estimated SWCC-w from the Zhou *et al.* (2014) equation does not merge into the virgin drying line, while the Tarantino (2009) equations are unable to match the residual drying line for the sand specimen.

Another verification of the proposed equation was carried out for the kaolin specimens (specimen 1 and specimen 2) as shown in Fig. 3. Specimen 1 was used to obtain the parameters in the proposed equation. The SWCC-w of specimen 2 was estimated. It is shown in Fig. 3 that the Zhou *et al.* (2014) and Tarantino (2009) equations manage to estimate the SWCC-w of specimen 2 very well, but merge into the virgin drying line at very high matric suction (near to the residual matric suction). In contrast, the estimated SWCC-w from the proposed equation merges into the virgin drying line near the intersection between the initial drying line and the virgin drying line.

The verification of the proposed equation was also carried out using data from Salager *et al.* (2010), Nishimura *et al.* (2011), Romero *et al.* (1999) and Gallage *et al.* (2013). Salager *et al.* (2010) tested a clayey silty sand which consisted of 72% sand, 18% silts and 10% clay and $G_s = 2{\cdot}65$ to investigate the effect of density on SWCC. The specimens were compacted into five different densities with initial void ratios of 1·01, 0·86, 0·68, 0·55 and 0·44. Nishimura *et al.* (2011) investigated the SWCC of Toyoura sand with $G_s = 2{\cdot}64$, $\rho_{\text{dry-max}} = 1{\cdot}645$ g/cm^3 and $\rho_{\text{dry-min}} = 1{\cdot}335$ g/cm^3. The Toyoura sand was compacted into five different relative densities (0·39, 11·6, 54·9, 63 and 73·3). Table 4 shows that the values of saturated volumetric water content θ_s which were measured by Nishimura *et al.* (2011) are not consistent with the reported relative density. Therefore, θ_s was recalculated by using the relative density of the specimens, and the subsequent volumetric water content at different matric suction θ_w was calculated based on the change in volumetric water content. Romero *et al.* (1999) investigated statically compacted natural Boom clay powder, with a liquid limit of 56%, plastic limit of 29% and 50% of the particles less than 2 μm. The SWCC-w of the Boom clay was obtained under two initial dry densities of 13·7 kN/m^3 (S13·7) and 16·7 kN/m^3 (S16·7). The last two soils from Gallage *et al.* (2013) are Edosaki sand (E12·2 and E13·5) with $G_s = 2{\cdot}75$ and Chiba soil (C12·2 and C13·5) with $G_s = 2{\cdot}72$, which were compacted into two different densities of 12·2 kN/m^3 (E12·2 and C12·2) and 13·5 kN/m^3 (E13·5 and C13·5).

Using the above-mentioned soils, the proposed equation, Zhou *et al.* (2014) equation and Tarantino (2009) equation were compared. The SWCC-w of the clayey silty sand specimen with initial void ratio = 1·01, Toyoura sand specimen with $D_r = 0{\cdot}39$, Boom clay with dry density 13·7 kN/m^3 (S13·7), Edosaki sand and Chiba soil with dry density 12·2 kN/m^3 (E12·2 and C13·5) were used to determine the parameters and the other SWCCs were estimated.

Only the SWCC-w curves for the clayey silty sand and the Boom clay are plotted in Fig. 4 for illustration purposes. The comparisons between the proposed equation and the other two equations for all of the soils are shown in Fig. 5. Table 5 gives a quantitative evaluation between the three equations by using the root-mean-square error (RMSE) between the measured water content and the estimated water content from both the calibrated and the estimated

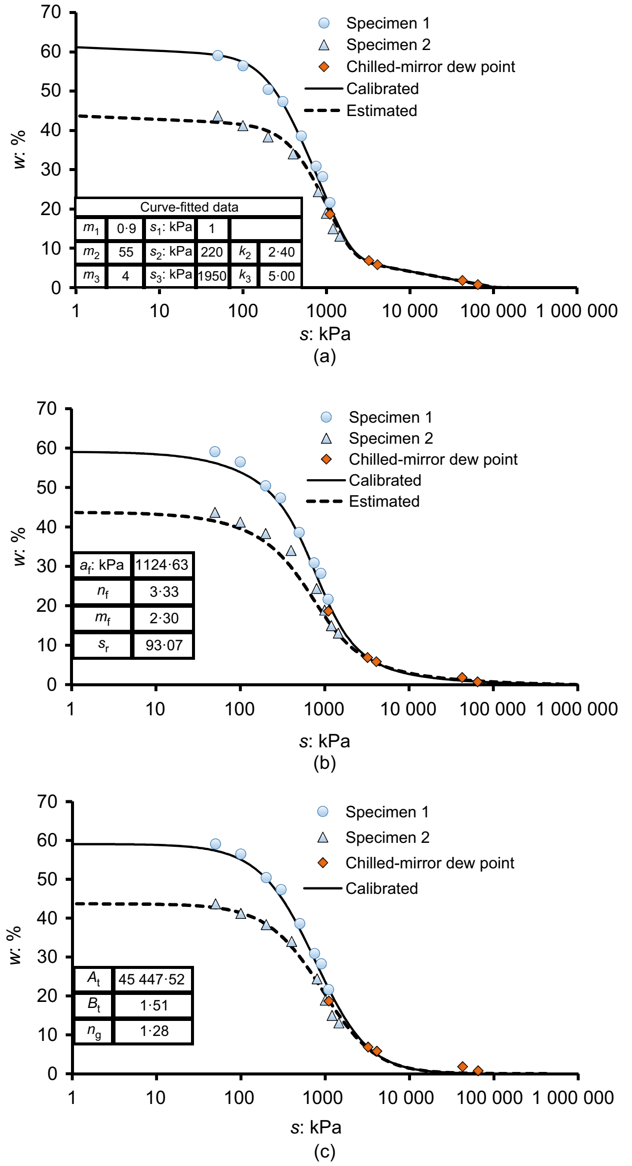

Fig. 3. SWCC-w of kaolin specimens: (a) proposed equation; (b) Zhou *et al.* (2014) equation; (c) Tarantino (2009) equation

Table 4. Toyoura sand properties

D_r: %	$\theta_{\text{s-measured}}$	$\theta_{\text{s-calculated}}$
0·39	40·6	49·39
11·6	41·6	48·30
54·9	37·6	43·60
63	39·5	42·62
73·3	40	41·33

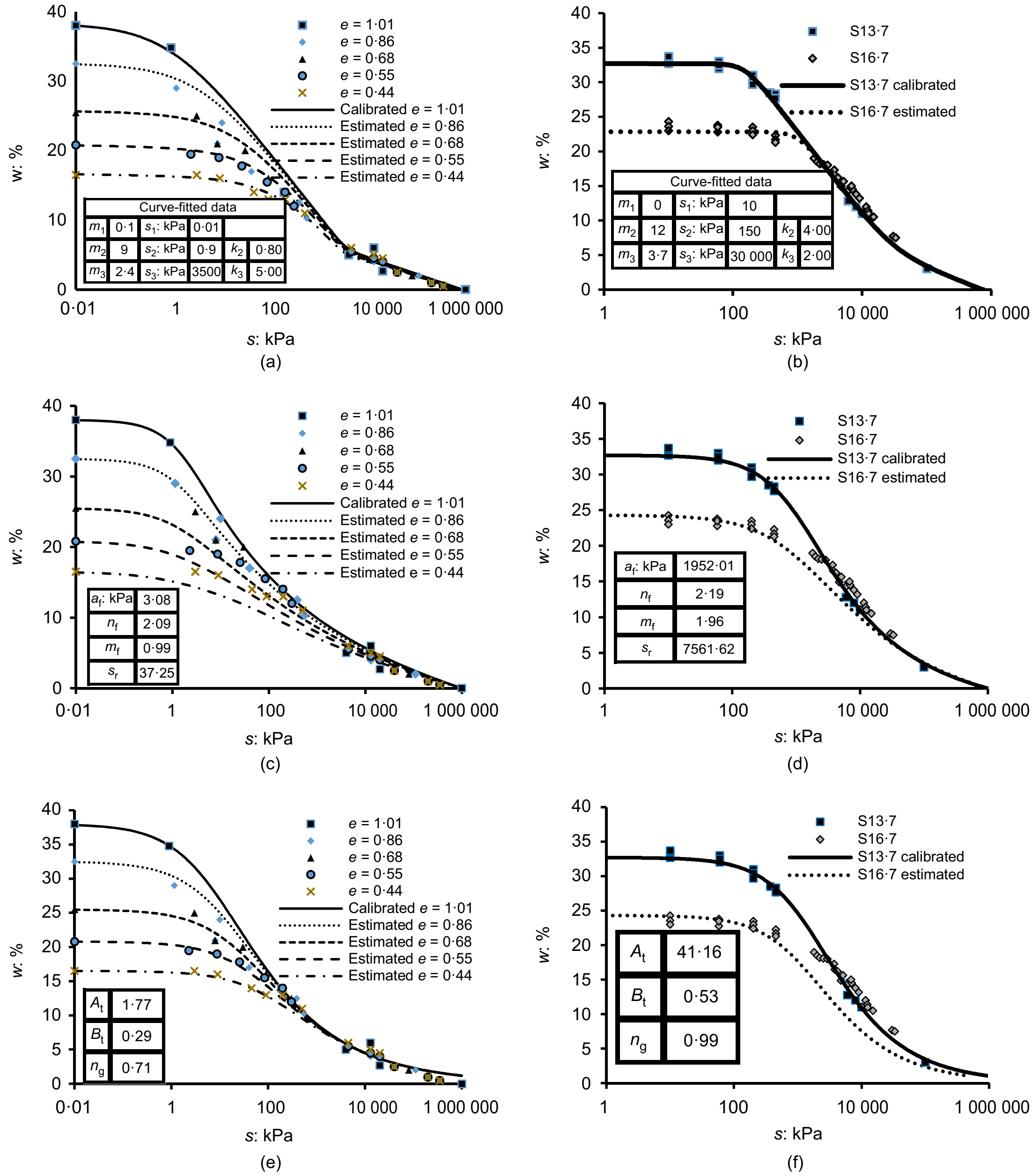

Fig. 4. Estimation of SWCC-w for clayey silty sand and Boom clay: (a) clayey silty sand (proposed equation); (b) Boom clay (proposed equation); (c) clayey silty sand (Zhou *et al.* (2014) equation); (d) Boom clay (Zhou *et al.* (2014) equation); (e) clayey silty sand (Tarantino (2009) equation); (f) Boom clay (Tarantino (2009) equation)

curve. The RMSE is defined as

$$\mathrm{RMSE} = \sqrt{\frac{\sum_{i=1}^{n}\left(w_{\text{measured-}i} - w_{\text{estimated-}i}\right)^2}{n}} \tag{13}$$

where i is the ith data point, n is the number of data points for all the SWCC (calibrated and estimated), $w_{\text{measured-}i}$ is the measured water content at the ith data point, $w_{\text{estimated-}i}$ is the estimated water content at the ith data point. The smaller the value of RMSE, the better the agreement between estimated and measured data. Figure 5 shows that the proposed equation performed better in most of the cases except for clayey silty sand and kaolin, where the Tarantino (2009) equation performed better. For the kaolin, the difference in RMSE between the Tarantino (2009) equation and the proposed equation is very small. However, the Tarantino (2009) equation causes the estimated SWCC-w to merge into the virgin drying line at a higher matric suction. Based on this evaluation, it appears that the Tarantino (2009) equation is good at estimating the SWCC-w of fine-grained soils where there is a smooth transition between two segments. However, when there is an abrupt change in slope between two segments (which is common in coarse-grained soils), the Tarantino (2009) equation tends to give an incorrect estimate and seems unable to give a good prediction for the low water content range. The Zhou *et al.* (2014) equation gives the worst performance for all soils evaluated and thus is not recommended to be used in estimating SWCC-w. Overall, the proposed equation gave the best performance and is thus suitable for any type of soil.

The slopes and intersection points of the SWCC-w are related to the compressibility and stress history of the soil (Pham & Fredlund, 2008). Thus, it is possible to correlate the slopes and the intersection points of the SWCC-w with unloading–reloading index, compression index and preconsolidation pressure. However, to correlate the SWCC-w with

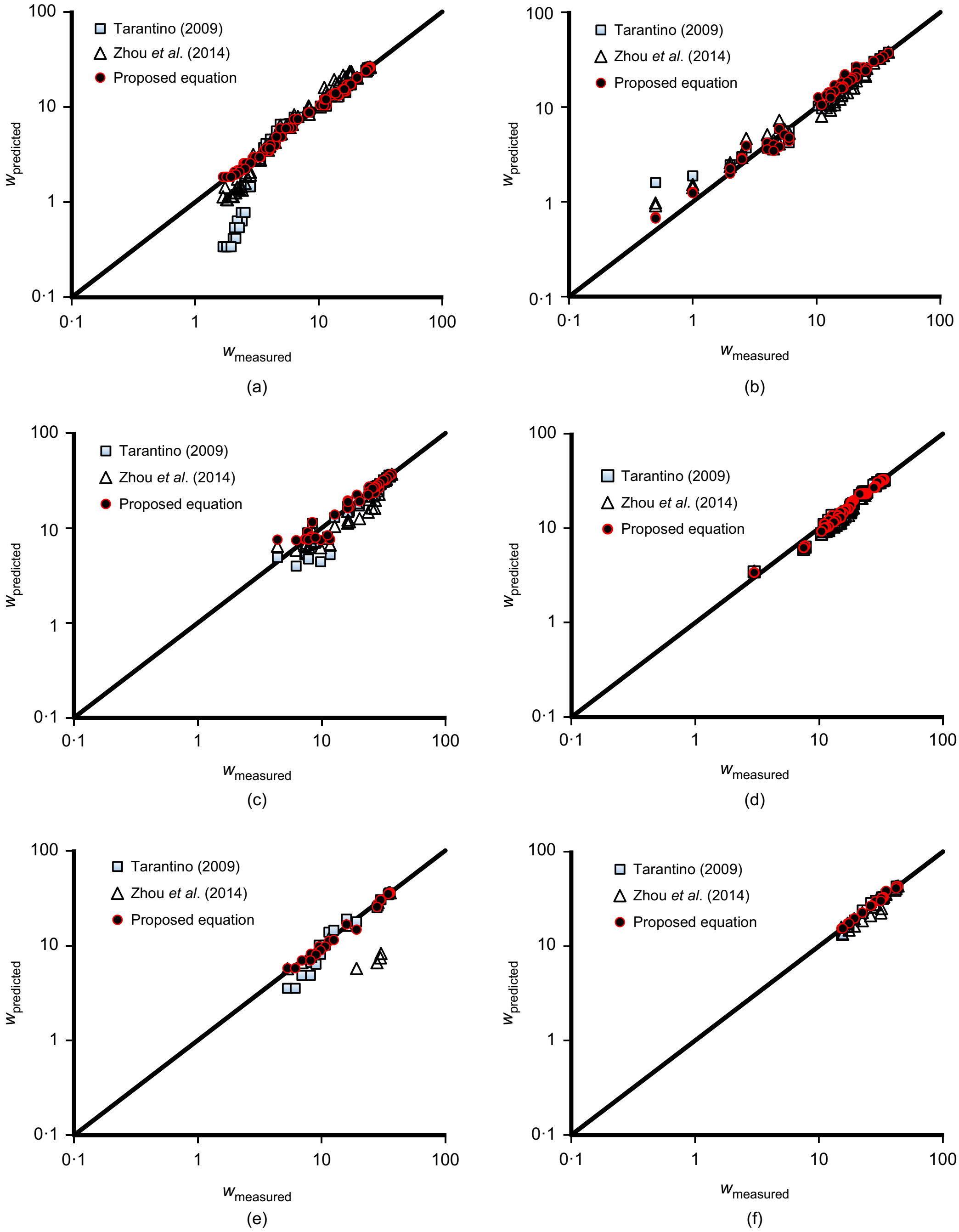

Fig. 5. Comparison of proposed equation with other equations: (a) sand specimen; (b) clayey silty sand (Salager *et al.*, 2010); (c) Toyoura sand (Nishimura *et al.*, 2011); (d) Boom clay (Romero *et al.*, 1999); (e) Edosaki sand (Gallage *et al.*, 2013); (f) Chiba soil (Gallage *et al.*, 2013)

Table 5. Comparison of proposed equation with other equations

Specimen	RMSE		
	Zhou *et al.* (2014)	Tarantino (2009)	Proposed equation
Sand (present study)	1·830	0·957	0·500
Kaolin (present study)	1·682	1·328	1·342
Clayey silty sand (Salager *et al.*, 2010)	1·893	1·118	1·515
Toyoura sand (Nishimura *et al.*, 2011)	4·047	2·393	1·797
Boom clay (Romero *et al.*, 1999)	1·839	1·288	0·944
Edosaki sand (Gallage *et al.*, 2013)	2·012	1·908	1·302
Chiba soil (Gallage *et al.*, 2013)	2·991	1·645	0·965

the compressibility and the stress history of the soil requires compression tests to be performed on specimens identical to those used to obtain the SWCC-w. This is outside the scope of the present study.

CONCLUSION

The density of soil only affects the initial portion of the gravimetric based soil-water characteristic curve (SWCC-w). In this note, a new equation to account for the effect of density on SWCC-w by using only one SWCC-w was proposed. It was evaluated using experimental data and showed a good performance compared to the other equations available. The proposed equation will be extended to bimodal SWCC-w in future.

ACKNOWLEDGEMENT

The first author acknowledges the research scholarship provided by Nanyang Technological University.

NOTATION

AEV_f air-entry value after changes in density
AEV_0 air-entry value prior to change in density
D_r relative density
e void ratio
e_{max} maximum void ratio of coarse-grained soils
e_{min} minimum void ratio of coarse-grained soils
e_0 initial void ratio
G_s specific gravity
k_i curvature parameter between segment i and segment $i-1$
m_i slope of segment i
m_1 slope of initial drying line
m_2 slope of virgin drying line
m_3 slope of residual drying line
n number of segments in soil-water characteristic curve
n_0 initial porosity
S_r degree of saturation
s matric suction
s_i matric suction at intersection between segment i and segment $i-1$
s_1 matric suction at saturated gravimetric water content
s_2 matric suction at intersection between initial drying line and virgin drying line
s_3 matric suction at intersection between virgin drying line and residual drying line
T_i transition function which represent linear segment i
w gravimetric water content
$w_{s,0}$ saturated gravimetric water content prior to change in density
$w_{s,f}$ saturated gravimetric water content after changes in density
w_{sat} or w_s saturated gravimetric water content
θ_s saturated volumetric water content
θ_w volumetric water content

REFERENCES

ASTM (2008). ASTM D6836-02: Standard test method for determination of soil water characteristic curve for desorption using hanging column, pressure extractor, chilled mirror hygrometer, or centrifuge. West Conshohocken, PA, USA: ASTM International.

Burger, C. A. & Shackelford, C. D. (2001). Evaluating dual porosity of pelletized diatomaceous earth using bimodal soil-water characteristic curve functions. *Can. Geotech. J.* **38**, No. 1, 53–66.

Chin, K. B., Leong, E. C. & Rahardjo, H. (2010). A simplified method to estimate the soil-water characteristic curve. *Can. Geotech. J.* **47**, No. 12, 1382–1400.

Durner, W. (1994). Hydraulic conductivity estimation for soils with heterogeneous pore structure. *Water Resources Res.* **30**, No. 2, 211–223.

Fredlund, D. G. & Rahardjo, H. (1993). *Soil mechanics for unsaturated soils.* New York, NY, USA: Wiley.

Fredlund, D. G. & Xing, A. (1994). Equations for the soil-water characteristic curve. *Can. Geotech. J.* **31**, No. 4, 521–532.

Gallage, C., Kodikara, J. & Uchimura, T. (2013). Laboratory measurement of hydraulic conductivity functions of two unsaturated sandy soils during drying and wetting processes. *Soils Found.* **53**, No. 3, 417–430.

Gallipoli, D., Wheeler, S. J. & Karstunen, M. (2003). Modelling the variation of degree of saturation in a deformable unsaturated soil. *Géotechnique* **53**, No. 1, 105–111, http://dx.doi.org/10.1680/geot.2003.53.1.105.

Gitirana, G. F. N. Jr & Fredlund, D. (2004). Soil-water characteristic curve equation with independent properties. *J. Geotech. Geoenviron. Engng* **130**, No. 2, 209–212.

Huang, S., Barbour, S. L. & Fredlund, D. G. (1998). Development and verification of a coefficient of permeability function for a deformable unsaturated soil. *Can. Geotech. J.* **35**, No. 3, 411–425.

Jotisankasa, A., Ridley, A. & Coop, M. (2007). Collapse behavior of compacted silty clay in suction-monitored oedometer apparatus. *J. Geotech. Geoenviron. Engng* **133**, No. 7, 867–877.

Li, X. (2009). *Dual-porosity structure and bimodal hydraulic property functions for unsaturated coarse granular soils.* PhD thesis, Hong Kong University of Sciene and Technology, Hong Kong.

Li, X., Li, J. H. & Zhang, L. M. (2014). Predicting bimodal soil–water characteristic curves and permeability functions using physically based parameters. *Comput. Geotech.* **57**, 85–96.

Mallants, D., Tseng, P. H., Toride, N., Tinunerman, A. & Feyen, J. (1997). Evaluation of multimodal hydraulic functions in characterizing a heterogeneous field soil. *J. Hydrol.* **195**, No. 1–4, 172–199.

Nishimura, T., Koseki, J. & Rahardjo, H. (2011). Effect of density for sand on hysteresis in soil-water characteristic curve. In *Proceedings of unsaturated soils: theory and practice* (eds A. Jotisankasa, A. Sawangsuriya, S. Soralump and W. Mairaing). Bangkok, Thailand: Geotechnical Engineering Research and Development Centre, Department of Civil Engineering, Kasetsart University.

Nuth, M. & Laloui, L. (2008). Advances in modelling hysteretic water retention curve in deformable soils. *Comput. Geotech.* **35**, No. 6, 835–844.

Othmer, H., Diekkruger, B. & Kutilek, M. (1991). Bimodal porosity and unsaturated hydraulic conductivity. *Soil Sci.* **152**, No. 3, 139–149.

Pham, H. Q. & Fredlund, D. G. (2008). Equations for the entire soil-water characteristic curve of a volume change soil. *Can. Geotech. J.* **45**, No. 4, 443–453.

Romero, E., Gens, A. & Lloret, A. (1999). Water permeability, water retention and microstructure of unsaturated compacted Boom clay. *Engng Geol.* **54**, No. 1–2, 117–127.

Ross, P. J. & Smettem, K. R. J. (1993). Describing soil hydraulic properties with sums of simple functions. *Soil Sci. Soc. Am. J.* **57**, No. 1, 26–29.

Salager, S., El Youssoufi, M. S. & Saix, C. (2010). Definition and experimental determination of a soil-water retention surface. *Can. Geotech. J.* **47**, No. 6, 609–622.

Salager, S., Ferrari, A., Nuth, M. & Laloui, L. (2011). Investigations on water retention behaviour of deformable soils. In *Proceedings of unsaturated soils* (eds E. E. Alonso and A. Gens), pp. 485–490. London, UK: CRC Press, Taylor & Francis Group.

Satyanaga, A., Rahardjo, H., Leong, E. C. & Wang, J. Y. (2013). Water characteristic curve of soil with bimodal grain-size distribution. *Comput. Geotech.* **48**, 51–61.

Sheng, D. & Zhou, A. N. (2011). Coupling hydraulic with mechanical models for unsaturated soils. *Can. Geotech. J.* **48**, No. 5, 826–840.

Smettem, K. R. J. & Kirkby, C. (1990). Measuring the hydraulic properties of a stable aggregated soil. *J. Hydrol.* **117**, No. 1–4, 1–13.

Tarantino, A. (2009). A water retention model for deformable soils. *Géotechnique* **59**, No. 9, 751–762, http://dx.doi.org/10.1680/geot.7.00118.

Tarantino, A. & Tombolato, S. (2005). Coupling of hydraulic and mechanical behaviour in unsaturated compacted clay. *Géotechnique* **55**, No. 4, 307–317, http://dx.doi.org/10.1680/geot.2005.55.4.307.

Van Genuchten, M. T. (1980). A closed-form equation for predicting the hydraulic conductivity of unsaturated soils. *Soil Sci. Soc. Am. J.* **44**, No. 5, 892–898.

Wijaya, M. & Leong, E. C. (2016). Equation for unimodal and bimodal soil–water characteristic curves. *Soils Found.* **56**, No. 2, 291–300.

Wijaya, M., Leong, E. C. & Rahardjo, H. (2015). Effect of shrinkage on air-entry value of soils. *Soils Found.* **55**, No. 1, 166–180.

Williams, P. J. (1982). *The surface of the earth, an introduction to geotechnical science*. New York, NY, USA: Longman Inc.

Wilson, G. V., Jardine, P. M. & Gwo, J. P. (1992). Modeling the hydraulic properties of a multiregion soil. *Soil Sci. Soc. Am. J.* **56**, No. 6, 1731–1737.

Zhang, L. M. & Chen, Q. (2005). Predicting bimodal soil–water characteristic curves. *J. Geotech. Geoenviron. Engng* **131**, No. 5, 666–670.

Zhou, A. N., Sheng, D. & Carter, J. P. (2012). Modelling the effect of initial density on soil-water characteristic curves. *Géotechnique* **62**, No. 8, 669–680, http://dx.doi.org/10.1680/geot.10.P.120.

Zhou, W. H., Yuen, K. V. & Tan, F. (2014). Estimation of soil–water characteristic curve and relative permeability for granular soils with different initial dry densities. *Engng Geol.* **179**, 1–9.